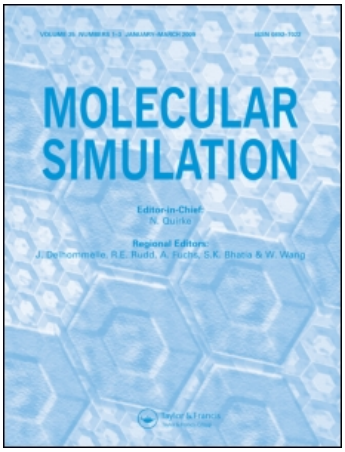

Molecular Simulation
Publication details, including instructions for authors and subscription information:
http://www.informaworld.com/smpp/title~content=t713644482

Calculating Free Energies Using a Scaled-Force Molecular Dynamics Algorithm

Eric Darve[a]; Michael A. Wilson; Andrew Pohorille
[a] Center for Turbulence Research, Stanford University, Stanford, CA

Online publication date: 26 October 2010

To cite this Article Darve, Eric , Wilson, Michael A. and Pohorille, Andrew(2002) 'Calculating Free Energies Using a Scaled-Force Molecular Dynamics Algorithm', Molecular Simulation, 28: 1, 113 — 144
To link to this Article: DOI: 10.1080/08927020211975
URL: http://dx.doi.org/10.1080/08927020211975

Molecular Simulation, 2002, Vol. 28(1–2), pp. 113–144

Taylor & Francis
Taylor & Francis Group

CALCULATING FREE ENERGIES USING A SCALED-FORCE MOLECULAR DYNAMICS ALGORITHM

ERIC DARVE[a], MICHAEL A. WILSON[b,c] and ANDREW POHORILLE[b,c,*]

[a]*Center for Turbulence Research, Stanford University, Stanford, CA 94305;* [b]*Exobiolgy Branch, MS 239-4, NASA Ames Research Center, Moffett Field, CA 94035;* [c]*Dept. of Pharmaceutical Chemistry, University of California, San Francisco, CA 94143*

(Received November 2000; accepted February 2001)

We propose and test a family of methods to calculate the free energy along a generalized coordinate, ξ, based on computing the force acting on this coordinate. First, we derive a formula that connects the free energy in unconstrained simulations with the force of constraint that can be readily calculated numerically. Then, we consider two methods, which improve the efficiency of the free energy calculation by yielding uniform or nearly uniform sampling of ξ. Both rely on modifying the force acting on ξ. In one method, this force is replaced by a force with zero mean and ξ is advanced quasistatically. In the second method, the force is augmented adaptively by a biasing force. We provide formulas for calculating the free energy of the unmodified system from the forces acting in these modified, non-Hamiltonian systems. Using conformational transitions in 1,2-dichloroethane as a test case, we show that both methods perform very well.

Keywords: Free energy; Molecular dynamics; Force of constraint; Adaptive force; Quasi-static approximation

1. INTRODUCTION

One common objective of molecular simulations in chemistry and biology is to calculate the free energy difference between different states of a system of interest. Examples of problems that have such an objective are calculations of receptor-ligand or protein-drug interactions, conformational preferences

*Corresponding author.

ISSN: 0892-7022 DOI: 10.1080/08927020290004412

of flexible molecules, associations of molecules in response to hydrophobic and electrostatic interactions or partition of molecules between immiscible liquids. Another common objective is to describe the evolution of a system towards a low energy (possibly the global minimum energy), "native" state. Perhaps the best example of such a problem is the folding of proteins or short RNA molecules.

Both types of problems share the same difficulty. Often, different states of the system are separated by high energy barriers, which implies that transitions between these states are rare events. This, in turn, can greatly impede exploration of phase space. In some instances this can lead to "quasi non-ergodicity", whereby a part of phase space is inaccessible on timescales of the simulation.

A host of strategies have been developed to improve the efficiency of sampling phase space [1–4]. For example, some Monte Carlo techniques involve large steps, which move the system between low-energy regions in phase space without the need for sampling configurations corresponding to energy barriers [5, 6]. Most strategies, however, rely on modifying the probabilities of sampling low and high-energy regions, such that transitions between states of interest are encouraged. Perhaps the simplest implementation of this strategy is to increase the temperature of the system. This approach was successfully used to identify denaturation pathways in several proteins [7–9], but it is clearly not applicable to protein folding. It is also not a successful method for determining free energy differences. Finally, the approach is likely to fail for systems with co-existing phases, such as water-membrane systems, because it may lead to spontaneous mixing. A similar difficulty may be encountered in any method relying on global modifications of phase space.

A promising, new technique is the multicanonical Monte Carlo method [10, 11]. In this algorithm, Boltzmann weighted sampling is substituted by sampling from a uniform energy probability distribution. This means that a multicanonical simulation corresponds to a random walk in one-dimensional energy space and, therefore, the system does not experience energy barriers. Since multicanonical weights are not known initially, they have to be estimated in the first step of the simulations. The multicanonical Monte Carlo method appears to be particularly suitable to study helix-coil transition in proteins, because a single simulation can provide information about both the low-temperature, helical state and the high-temperature, disordered state.

Many problems of chemical or biological interest can be formulated in terms of the evolution of a system along a small number of slow degrees of

freedom in the potential of mean force exerted by the remaining coordinates. An effective strategy in this case is to add a biasing potential to the Hamiltonian which lowers the free energy barriers in this reduced representation [12, 13]. Identifying the slow degrees of freedom is not always easy, especially if a formally defined reaction coordinate is sought. In many instances, however, our intuitive understanding of the problem can successfully guide us in this process. For example, the transport of ions and small molecules across membranes can be well described by calculating the potential of mean force associated with moving the center of mass of the solute in the direction perpendicular to the membrane [14–16]. In another example, the folding of peptides or small, single-domain proteins can be studied by selecting ϕ, ψ and, possibly, some χ angles as slow degrees of freedom [17].

The method of biasing potentials has several important advantages. First, using a reduced representation is very helpful in planning the simulations and analyzing their results. In fact, it can be argued that, precisely for this reason, it is extremely useful to identify the slow degrees of freedom from the very beginning. Second, if the motion along only a few such degrees of freedom is modified, the chances for correctly identifying the pathways along which the system evolves improve markedly. The approach also has a serious disadvantage. To design a useful biasing potential, a good, initial guess about the shape of the potential of mean force is required. If no such guess is available, the approach may turn into a frustrating experience. Unfortunately, correctly estimating the potential of mean force is often quite difficult because it depends on several contributions of different origins, such as solute–solvent interactions, solvent reorganization and interactions between solute atoms separated by many bonds, but close in space.

In this paper, we present a new approach to the problem of efficient sampling of phase space, based on the molecular dynamics (MD) algorithm in the canonical ensemble. As in the methods of biasing potential, it requires the initial identification of slow degrees of freedom. It does not, however, suffer from the main disadvantage of these methods: no prior assumptions about the shape of the potential of mean force are needed. Even without these assumptions, the free energy differences between states in the reduced phase space can be calculated very efficiently.

We prove that the derivative of the free energy along a selected generalized degree of freedom can be expressed by an average force, which is a function of this coordinate, and its derivatives with respect to time and positions of the particles. Thus, it can be easily calculated numerically. If this force is scaled by $0 < \alpha < 1$ or completely eliminated and substituted by another, suitably chosen force sampling of the generalized coordinate

improves markedly. To underscore this feature we call our approach the Scaled Force Method (SFM). Even though the new force acting on the selected coordinate is not, in general, derived from a Hamiltonian, it is still possible, under appropriate conditions, to calculate the potential of mean force along the selected coordinate in the unmodified system.

In the next section, we present the main idea and the implementation of the method. This is followed by an example of how the method works. As the test case, we selected conformational transition of 1,2-dichloroethane in water, which has been studied extensively in various environments [18–25]. The main body of the paper closes with the discussion of the method in the context of other approaches, its application to studies of dynamical processes and the outline of future work. The details of the required modification to the standard MD algorithm are given in the appendix.

2. THEORY

2.1. Basic Ideas

Consider a system of N particles characterized by their positions, $\boldsymbol{x}_1, \ldots, \boldsymbol{x}_N$, and momenta $\boldsymbol{p}_{\boldsymbol{x}_1}, \ldots, \boldsymbol{p}_{\boldsymbol{x}_N}$. Motion of the system is described by the Hamiltonian H:

$$H(\boldsymbol{x}, \boldsymbol{p}_x) = \frac{1}{2} \sum_i \frac{\boldsymbol{p}_{\boldsymbol{x}_i}^2}{m_i} + \Phi(\boldsymbol{x}) \tag{1}$$

where $\boldsymbol{x}$, $\boldsymbol{p}_x$ are vectors of the Cartesian coordinates and momenta, respectively.

We assume that we are interested in the free energy changes along a slow degree of freedom, ξ. The extension to a larger number of slow, generalized coordinates will not be described in this paper. A conventional method of calculating the free energy $A(\xi)$ as a function of ξ (the potential of mean force along ξ) is to obtain the probability density, $P(\xi)$, of finding the system in the states corresponding to different values of ξ, and to exploit the relation:

$$A(\xi) = -kT \ln P(\xi) + A_0 \tag{2}$$

where k is the Boltzmann constant, T is the temperature and A_0 is an arbitrary constant.

As has already been mentioned in the previous section, this approach may be inefficient if there are considerable free energy barriers along ξ. Then, the regions in phase space near the barriers will be visited only infrequently and the statistical precision of calculating $P(\xi)$ in these regions will suffer. However, the efficiency of sampling $P(\xi)$ may be greatly improved by modifying the Hamiltonian of the system by a biasing potential, $U_b(\xi)$, chosen such that sampling of ξ becomes more uniform. For the modified Hamiltonian

$$H'(\boldsymbol{x}, \boldsymbol{p}_x) = H(\boldsymbol{x}, \boldsymbol{p}_x) - U_b(\xi) \tag{3}$$

the potential of mean force is given by:

$$A(\xi) = -kT \ln P(\xi) + U_b(\xi) + A_0 \tag{4}$$

The optimal choice of $U_b(\xi)$, which yields the uniform distribution of $P(\xi)$, would be:

$$U_b(\xi) = A(\xi) \tag{5}$$

Of course in practice, this choice is not possible because it implies that the free energy is known before the simulation begins.

Alternatively, the free energy can be obtained from the same, unconstrained simulation by evaluating $(\partial \mathrm{A}/\partial \xi)$ in the full range of ξ. Recall that the probability density $P(\xi)$ can be defined in terms of an integral involving the Hamiltonian H and the delta function:

$$P(\xi) = \frac{\int_{\mathbb{R}^{6N}} \exp(-H/kT)\delta(\xi - \xi(\boldsymbol{x}))\, d\boldsymbol{x}\, d\boldsymbol{p}_x}{\int_{\mathbb{R}^{6N}} \exp(-H/kT)\, d\boldsymbol{x}\, d\boldsymbol{p}_x} \tag{6}$$

The delta function in the integral means that we integrate over all possible values of $\boldsymbol{x}$ and $\boldsymbol{p}_x$ with the constraint $\xi(\boldsymbol{x}) = \xi$. This set is a hypersurface, which we further denote S_ξ. There are $6N-1$ degrees of freedom on S_ξ. By using an appropriate change of variables involving generalized coordinates it is possible to define an infinitesimal element on the surface S_ξ which we denote $d\boldsymbol{s}$. Note that the Jacobian of the transformation from Cartesian to generalized degrees of freedom (coordinates + momenta) is 1. See the appendix for a concise justification (Section A.1 and Eq. (34)). We may write:

$$P(\xi) = \frac{\int_{S_\xi} \exp(-H/kT)\, d\boldsymbol{s}}{\int_{\mathbb{R}^{6N}} \exp(-H/kT)\, d\boldsymbol{x}\, d\boldsymbol{p}_x}$$

Differentiating Eq. (2) with respect to ξ we obtain

$$\frac{\partial A}{\partial \xi} = \frac{\int_{S_\xi} (\partial H/\partial \xi) \exp(-\beta H)\, d\boldsymbol{s}}{\int_{S_\xi} \exp(-\beta H)\, d\boldsymbol{s}} = \left\langle \frac{\partial H}{\partial \xi} \right\rangle_{S_\xi} = -\langle F_\xi \rangle_{S_\xi} \tag{7}$$

where $\beta = 1/kT$ and $\langle \rangle_{S_\xi}$ denotes the statistical average. As we will further show, the force acting on ξ, F_ξ, can be calculated in each step of the simulation, for example from the force of constraint using SHAKE or RATTLE algorithm [26, 27]. Once the average values of the force for the full range of ξ are calculated with sufficient statistical precision, $A(\xi)$ is obtained by integrating $\langle F_\xi \rangle_{S_\xi}$ over ξ.

In general, the method based on calculating the force along ξ in unconstrained simulations (which is distinct from calculating the force in constrained simulations [28]), defined by Eq. (7), has no obvious advantages over the method based on calculating the probability distribution (Eq. (2)). Its utility is that it provides a framework to consider new methods for calculating the free energy. The goal of these methods is to achieve uniform or nearly uniform sampling of ξ without prior knowledge of the biasing potential. In SFM, uniform sampling is obtained by decoupling ξ from the other degrees of freedom and advancing it using a force that yields a uniform probability density. One choice for advancing ξ in this manner is provided by the Langevin equation. We will prove that if the motion of ξ is quasistatic, then the average of $-F_\xi$ converges to $(\partial A/\partial \xi)$. The advantage of using the Langevin equation is that the range of applicability of quasistatic approximation can be systematically studied simply by changing the diffusion coefficient. Other stochastic or deterministic algorithms are possible without introducing any complications to the general theory.

In the particular case when the additional (*i.e.*, Langevin) force is set to zero and the initial velocity of ξ is zero, ξ is constrained at its initial value. We then recover a result of den Otter and Briels [28].

We note that, in the canonical ensemble, H describes both the system of interest and the thermostat. In molecular dynamics simulations the thermostat is substituted by a small number of additional degrees of freedom and the Hamiltonian is replaced by a pseudo-Hamiltonian [29–31]. This, however, does not cause any additional complications in this case.

Nearly uniform sampling along ξ can be also accomplished without appealing to the quasistatic approximation. When a biasing potential is used, energy barriers can be reduced by adding a biasing force equal to $(\partial U_b/\partial \xi)$. If the optimal biasing potential were used (see Eq. (5)) the biasing force

would be equal to

$$\frac{\partial U_b}{\partial \xi} = \frac{\partial A}{\partial \xi} = -\langle F_\xi \rangle_{S_\xi}$$

Instead of using $-\langle F_\xi \rangle_{S_\xi}$, which is not known, we employ its current estimate as the biasing force. We call this method the Adaptive Biasing Force method. In this method, the biasing force at location ξ_0 is equal to $-\langle F_\xi \rangle^{(n)}_{S_{\xi_0}}$ where

$$\langle F_\xi \rangle^{(n)}_{S_{\xi_0}} = \frac{1}{n} \sum_{i=1}^{n} F_\xi^i \tag{8}$$

and n is the number of samples in the bin around ξ_0. At the beginning of the computation when the number of samples is very small, $\langle F_\xi \rangle^{(n)}_{S_\xi}$ vary considerably. However, it converges fairly quickly to its limit. Then, the system can be considered as described by the Hamiltonian H augmented by a small, time-dependent, slowly changing term, which converges to zero as time goes to infinity. In these circumstances, configurations of the system are also, to a good approximation, generated from the appropriate thermodynamic ensemble. If this is the case, then $\langle F_\xi \rangle^{(n)}_{S_{\xi_0}}$ converges to $-(\partial A/\partial \xi)(\xi_0)$. Note that in this approach $P(\xi)$ will not be exactly constant. However, numerically observed deviations from uniformity are quite small.

The considerations presented above define the theoretical steps that still need to be done. First, we will derive the formula for $\langle F_\xi \rangle_{S_\xi}$ in a Hamiltonian system. Next, we will discuss the modifications to this formula that need to be made in the quasistatic approximation and define the equations of motion along ξ used in this work. Details of the algorithm are given in the appendix.

2.2. Thermodynamics Force

To properly define the partial derivative of A with respect to ξ it is necessary to introduce generalized coordinates $q_1, \ldots, q_{3N-1}$:

$$q_1 = q_1(x_1, \ldots, x_{3N})$$
$$q_{3N-1} = q_{3N-1}(x_1, \ldots, x_{3N})$$

such that for each set of values $(x_1, \ldots, x_{3N})$ there is a unique set of values $(\xi, q_1, \ldots, q_{3N-1})$. This means that:

$$x_1 = x_1(\xi, q_1, \ldots, q_{3N-1})$$
$$x_{3N} = x_{3N}(\xi, q_1, \ldots, q_{3N-1})$$

The derivative with respect to ξ can now be defined as the derivative computed with $q_1, \ldots, q_{3N-1}$ constant:

$$\frac{\partial}{\partial \xi} = \left(\frac{\partial}{\partial \xi} \right)_{q_1, \ldots, q_{3N-1}}$$

Finding a set of generalized coordinates is often difficult. Furthermore, $A(\xi)$ is independent of the choice of a particular set of these coordinates. This implies that the knowledge of generalized coordinates should not be required to calculate the free energy or its derivative. Thus, the aim of the following derivation is to transform the expression for the free energy such that explicit reference to generalized coordinates other than ξ is removed.

The Jacobian, J of the transformation from Cartesian to generalized coordinates is defined as:

$$J \stackrel{\text{def}}{=} \begin{pmatrix} (\partial \xi / \partial x_1) & (\partial \xi / \partial x_2) & \ldots & (\partial \xi / \partial x_N) \\ (\partial q_1 / \partial x_1) & (\partial q_1 / \partial x_2) & \ldots & (\partial q_1 / \partial x_N) \\ \ldots & \ldots & \ldots & \ldots \\ (\partial q_{3N-1} / \partial x_1) & (\partial q_{3N-1} / \partial x_2) & \ldots & (\partial q_{3N-1} / \partial x_{3N}) \end{pmatrix} \tag{9}$$

and its inverse is denoted by J^{-1}. We define the matrix Z as

$$Z \stackrel{\text{def}}{=} J M^{-1} J^t$$

where J^t is the transpose of the matrix J and M is the mass matrix:

$$M = \begin{pmatrix} m_1 & 0 & \ldots & 0 \\ 0 & m_2 & \ldots & 0 \\ \ldots & \ldots & \ldots & \ldots \\ 0 & 0 & \ldots & m_{3N} \end{pmatrix}$$

The matrix Z can be written:

$$Z = \begin{pmatrix} Z_\xi & 0 \\ 0 & Z_q \end{pmatrix}$$

where

$$Z_\xi \stackrel{\text{def}}{=} \sum_{k=1}^{3N} \frac{1}{m_k} \left(\frac{\partial \xi}{\partial x_k} \right)^2 \tag{10}$$

and Z_q is a $3N-1 \times 3N-1$ matrix.

In generalized coordinates the Hamiltonian of the system takes the form:

$$H(\xi, q, p_\xi, p_q) = \frac{1}{2} Z_\xi p_\xi^2 + \frac{1}{2} p_q^t Z_q p_q + \Phi(\xi, q) \tag{11}$$

and Eq. (7) becomes:

$$\frac{\partial A}{\partial \xi} = \left\langle \frac{1}{2} \frac{\partial Z_\xi}{\partial \xi} p_\xi^2 + \frac{1}{2} p_q^t \frac{\partial Z_q}{\partial \xi} p_q + \frac{\partial \Phi(\xi, q)}{\partial u \xi} \right\rangle_{S_\xi} \tag{12}$$

This formula is not very useful because it explicitly depends on $q_1, \ldots, q_{3N-1}$ and their conjugate momenta. In the next subsection this dependence will be eliminated.

2.3. Unconstrained Simulation

We introduce the following notations:

$$x_i' \stackrel{\text{def}}{=} \sqrt{m_i}\, x_i \tag{13}$$

$$p_{x_i}' \stackrel{\text{def}}{=} \frac{p_i}{\sqrt{m_i}} \tag{14}$$

$$\text{(modified Hessian of } \xi) \quad \mathcal{H} \stackrel{\text{def}}{=} \left(\frac{\partial^2 \xi}{\partial x_i' \partial x_j'} \right) = \left(\frac{1}{\sqrt{m_i m_j}} \frac{\partial^2 \xi}{\partial x_i \partial x_j} \right) \tag{15}$$

The symbol $\cdot$ denotes a dot product or a matrix-vector product depending on the context.

The momentum p_ξ is defined as the derivative of the Lagrangian $\mathcal{L}$ with respect to $\dot{\xi}$. As the Lagrangian $\mathcal{L}$ is defined by

$$\mathcal{L} = \frac{1}{2} \begin{pmatrix} \dot{\xi} \\ dq/dt \end{pmatrix}^t \cdot Z^{-1} \cdot \begin{pmatrix} \dot{\xi} \\ dq/dt \end{pmatrix} - \Phi(\xi, q)$$

the momentum p_ξ is equal to

$$p_\xi \stackrel{\text{def}}{=} \frac{\partial \mathcal{L}}{\partial \dot{\xi}} = \frac{\dot{\xi}}{Z_\xi} \tag{16}$$

Moreover we know that:

$$\frac{\partial H}{\partial \xi} = -\frac{dp_\xi}{dt} \tag{17}$$

By substituting Eq. (16) in Eq. (17) we obtain:

$$\frac{\partial H}{\partial \xi} = -\frac{\ddot{\xi}}{Z_\xi} + \frac{\dot{\xi}}{Z_\xi^2}\frac{dZ_\xi}{dt} \tag{18}$$

From the rules of derivation:

$$\frac{dZ_\xi}{dt} = \sum_i^{3N} \frac{\partial Z_\xi}{\partial x_i}\frac{dx_i}{dt} = \frac{\partial Z_\xi}{\partial \boldsymbol{x}'} \cdot \boldsymbol{p}'_x \tag{19}$$

Then, using Eqs. (18) and (19) and Definition (16), $(\partial H/\partial \xi)$ can be expressed as:

$$\frac{\partial H}{\partial \xi} = -\frac{\ddot{\xi}}{Z_\xi} + \frac{p_\xi}{Z_\xi}\frac{dZ_\xi}{\partial \boldsymbol{x}'} \cdot \boldsymbol{p}'_x \tag{20}$$

Recall that

$$\boldsymbol{p}_x = \boldsymbol{J}^t \begin{pmatrix} p_\xi \\ p_q \end{pmatrix} \tag{21}$$

Thus:

$$\int \exp(-\beta H)\frac{p_\xi}{Z_\xi}\frac{\partial Z_\xi}{\partial \boldsymbol{x}'} \cdot \boldsymbol{p}'_x \, dp_q = \int \exp(-\beta H)\frac{p_\xi}{Z_\xi}\frac{\partial Z_\xi}{\partial \boldsymbol{x}'} \cdot (\boldsymbol{J}')^t \begin{pmatrix} p_\xi \\ p_q \end{pmatrix} dp_q$$

where $\beta = 1/kT$. Since we integrate over p_q the only non-zero contribution is:

$$\int \exp(-\beta H)\frac{p_\xi}{Z_\xi}\frac{\partial Z_\xi}{\partial \boldsymbol{x}'} \cdot (\boldsymbol{J}')^t \begin{pmatrix} p_\xi \\ p_q \end{pmatrix} dp_q = \int \exp(-\beta H)\frac{p_\xi^2}{Z_\xi}\frac{\partial Z_\xi}{\partial \boldsymbol{x}'} \cdot \frac{\partial \xi}{\partial \boldsymbol{x}'} \, dp_q$$

using Definition (9) of J.

Finally using Definition (10) of Z_ξ and Definition (15) of $\mathcal{H}$:

$$\int \exp(-\beta H)\frac{p_\xi}{Z_\xi}\frac{\partial Z_\xi}{\partial \boldsymbol{x}'} \cdot \boldsymbol{p}'_x \, dp_q = 2\int \exp(-\beta H)\frac{p_\xi^2}{Z_\xi}\frac{\partial \xi}{\partial \boldsymbol{x}'} \cdot \mathcal{H} \cdot \frac{\partial \xi}{\partial \boldsymbol{x}'} \, dp_q \tag{22}$$

Now, we can compute the integral over p_ξ, and obtain, (see Eq. (11)) for the probability density of p_ξ:

$$\int p_\xi^2 \exp\left(-\frac{\beta}{2} Z_\xi p_\xi^2\right) dp_\xi = \frac{1}{\beta Z_\xi} \int \exp\left(-\frac{\beta}{2} Z_\xi p_\xi^2\right) dp_\xi \tag{23}$$

Gathering Eqs. (20), (22) and (23), we have proven that

$$\frac{\partial A}{\partial \xi} = \left\langle \frac{-1}{Z_\xi} \ddot{\xi} + \frac{2}{\beta Z_\xi^2} \frac{\partial \xi}{\partial \boldsymbol{x}'} \cdot \mathcal{H} \cdot \frac{\partial \xi}{\partial \boldsymbol{x}'} \right\rangle_{q, p_q, p_\xi} \tag{24}$$

$$\ddot{\xi} = -\frac{\partial \Phi}{\partial \boldsymbol{x}'} \cdot \frac{\partial \xi}{\partial \boldsymbol{x}'} + \boldsymbol{p}'_{\boldsymbol{x}} \cdot \mathcal{H} \cdot \boldsymbol{p}'_{\boldsymbol{x}} \tag{25}$$

where the indices $\langle\rangle_{q, p_q, p_\xi}$ mean that we average over q, p_q and p_ξ. Eq. (24) is very convenient numerically, because it involves only quantities that can be readily computed: $\ddot{\xi}$ and the first and second derivatives of ξ with respect to x.

We can now define the thermodynamics force as $\langle F_\xi \rangle$ where

$$F_\xi \stackrel{\text{def}}{=} \frac{1}{Z_\xi} \ddot{\xi} - \frac{2}{\beta Z_\xi^2} \frac{\partial \xi}{\partial \boldsymbol{x}'} \cdot \mathcal{H} \cdot \frac{\partial \xi}{\partial \boldsymbol{x}'} \tag{26}$$

2.4. Quasistatic Variations of ξ

In SFM the motion along ξ is decoupled from the rest of the system. Then, ξ is advanced in some manner that ensures uniform sampling of ξ, for example by using the Langevin equation of motion. In this new system, the free energy along ξ is no longer properly defined and Eq. (24) no longer applies. However, it is possible to compute the free energy of the original (unmodified) system, provided that the motion of ξ is quasistatic. This requires transforming Eq. (24). Deriving the appropriate formula for $(\partial A/\partial \xi)$ is the objective of this section.

Suppose that we run a MD simulation at fixed $\xi = \xi_0$. In the case of a Hamiltonian system, the probability density for (q, p_q, p_ξ) at $\xi = \xi_0$ is equal to $\exp(-\beta H_{\xi_0})$, where

$$H_{\xi_0}(q, p_q, p_\xi) = \frac{1}{2} Z_\xi p_\xi^2 + \frac{1}{2} p_q' Z_q p_q + \Phi_{\xi_0}(q) \tag{27}$$

However, when ξ is decoupled from other degrees of freedom and advanced quasistatically using an independent equation, we sample with a

probability equal to $\exp(-\beta H^*_{\xi_0})$, where

$$H^*_{\xi_0}(q, p_q, p_\xi) = K^{\text{ext}}(p_\xi) + \frac{1}{2} p_q^t Z_q p_q + \Phi_{\xi_0}(q) \tag{28}$$

The function K^{ext} depends on the equation of motion for ξ. If this is a diffusion (Langevin) equation

$$K^{\text{ext}}(p_\xi) = \frac{1}{2}\frac{T}{T_\xi} p_\xi^2$$

where T_ξ is the temperature used in the Langevin equation (see the appendix). Because we sample from a different probability distribution function it is not possible to use Eq. (24) directly. This difficulty can be solved by calculating analytically the integral over p_ξ in Eq. (24). To do so we first identify the terms which depend on p_ξ: the acceleration $\ddot{\xi}$ and the probability density. More specifically considering Eqs. (24) and (25), we need to calculate:

$$\int f_\xi \boldsymbol{p}'_{\boldsymbol{x}} \cdot \mathcal{H} \cdot \boldsymbol{p}'_{\boldsymbol{x}} \, dp_\xi$$

where $f_\xi = \exp(-(\beta/2) Z_\xi p_\xi^2)$.

Denoting $f_{p_q} = \exp((-\beta/2) p_q^t Z_q p_q)$ we have:

$$\int f_{p_q} \boldsymbol{p}'_{\boldsymbol{x}} \cdot \mathcal{H} \cdot \boldsymbol{p}'_{\boldsymbol{x}} \, dp_q = \int f_{p_q} \begin{pmatrix} p_\xi \\ p_q \end{pmatrix} \cdot J' \mathcal{H} (J')^t \cdot \begin{pmatrix} p_\xi \\ p_q \end{pmatrix} dp_q \tag{29}$$

$$= p_\xi^2 \frac{\partial \xi}{\partial \boldsymbol{x}'} \cdot \mathcal{H} \cdot \frac{\partial \xi}{\partial \boldsymbol{x}'} \int f_{p_q} \, dp_q + \int f_{p_q} p_q \cdot J'_q \mathcal{H} (J'_q)^t \cdot p_q \, dp_q \tag{30}$$

using Eqs. (17) and (18), and the fact that integration is performed over p_q.

Next we consider the integral over p_ξ and use Eq. (23):

$$\int f_\xi p_\xi^2 \, \frac{\partial \xi}{\partial \boldsymbol{x}'} \cdot \mathcal{H} \cdot \frac{\partial \xi}{\partial \boldsymbol{x}'} dp_\xi = \frac{1}{\beta Z_\xi} \frac{\partial \xi}{\partial \boldsymbol{x}'} \cdot \mathcal{H} \cdot \frac{\partial \xi}{\partial \boldsymbol{x}'} \int f_\xi \, dp_\xi \tag{31}$$

Using this equation, we observe that the following transformation is possible on statistical averages:

$$\left\langle \boldsymbol{p}'_{\boldsymbol{x}} \cdot \mathcal{H} \cdot \boldsymbol{p}'_{\boldsymbol{x}} + \left(\frac{1}{\beta Z_\xi} - \frac{\dot{\xi}^2}{Z_\xi^2} \right) \frac{\partial \xi}{\partial \boldsymbol{x}'} \cdot \mathcal{H} \cdot \frac{\partial \xi}{\partial \boldsymbol{x}'} \right\rangle_{q, p_q, p_\xi} = \langle \boldsymbol{p}'_{\boldsymbol{x}} \cdot \mathcal{H} \cdot \boldsymbol{p}'_{\boldsymbol{x}} \rangle_{q, p_q, p_\xi}$$

Further, using Eqs. (30) and (31)

$$\left\langle \boldsymbol{p}'_{\boldsymbol{x}} \cdot \mathcal{H} \cdot \boldsymbol{p}'_{\boldsymbol{x}} + \left(\frac{1}{\beta Z_\xi} - \frac{\dot{\xi}^2}{Z_\xi^2} \right) \frac{\partial \xi}{\partial \boldsymbol{x}'} \cdot \mathcal{H} \cdot \frac{\partial \xi}{\partial \boldsymbol{x}'} \right\rangle_{q,p_q,p_\xi}$$
$$= \left\langle \frac{1}{\beta Z_\xi} \frac{\partial \xi}{\partial \boldsymbol{x}'} \cdot \mathcal{H} \cdot \frac{\partial \xi}{\partial \boldsymbol{x}'} + p_q \cdot J'_q \mathcal{H} (J'_q)^t \cdot p_q \right\rangle_{q,p_q,p_\xi}$$

We have proven the following result:

$$\int \exp(-\beta H_{\xi_0}) F_\xi d_q d_{p_q} d_{p_\xi} = \int \exp(-\beta H_{\xi_0}) F_\xi^{(2)} d_q d_{p_q} d_{p_\xi}$$

with

$$F_\xi^{(2)} = \frac{1}{Z_\xi} \ddot{\xi} - \left(\frac{1}{\beta} + \frac{\dot{\xi}^2}{Z_\xi} \right) \frac{1}{Z_\xi^2} \frac{\partial \xi}{\partial \boldsymbol{x}'} \cdot \mathcal{H} \cdot \frac{\partial \xi}{\partial \boldsymbol{x}'}$$

(see Eq. (26) for the definition of F_ξ). Moreover $\int f_{p_q} F_\xi^{(2)} \, dp_q$ is independent of p_ξ. Thus, we have removed the dependence of the average force on p_ξ. This is a desirable result because the dependence on p_ξ changes with implementation of the quasistatic process. Thus we can conclude:

$$\int dp_\xi \, f_\xi \int dp_q \, f_{p_q} F_\xi^{(2)} = \int dp_q \, f_{p_q} F_\xi^{(2)} \times \int dp_\xi \, \exp\left(-\frac{\beta}{2} Z_\xi p_\xi^2 \right) \propto \frac{1}{\sqrt{Z_\xi}} \int dp_q \, f_{p_q} F_\xi^{(2)}$$

We proved that when ξ is decoupled and moves quasistatically, the following equation applies:

$$\frac{\partial A}{\partial \xi} = \frac{\langle (1/\sqrt{Z_\xi}) F_\xi^{(2)} \rangle_{q,p_q}}{\langle (1/\sqrt{Z_\xi}) \rangle_{q,p_q}} = \frac{\langle (-1/Z_\xi^{3/2}) \ddot{\xi} + (1/Z_\xi^{5/2})((1/\beta) + (\dot{\xi}^2/Z_\xi))(\partial \xi/\partial \boldsymbol{x}') \cdot \mathcal{H} \cdot (\partial \xi/\partial \boldsymbol{x}') \rangle_{q,p_q}}{\langle (1/\sqrt{Z_\xi}) \rangle_{q,p_q}} \tag{32}$$

where A is the free energy of the original system.

2.5. Constrained Simulation

The case of the constrained simulation is a corollary of the previous result. It is a particular case of a "quasistatic" motion where the velocity of ξ is zero. In this case $F_\xi^{(2)}$ is simply equal to:

$$F_\xi^{(2)} = \frac{-1}{Z_\xi}\ddot{\xi} + \frac{1}{\beta}\frac{1}{Z_\xi^2}\frac{\partial \xi}{\partial \boldsymbol{x}'} \cdot \mathcal{H} \cdot \frac{\partial \xi}{\partial \boldsymbol{x}'}$$

Thus the complete expression for $(\partial A/\partial \xi)$ is

$$\frac{\partial A}{\partial \xi} = \frac{\langle (-1/Z_\xi^{3/2})\ddot{\xi} + (1/\beta)(1/Z_\xi^{5/2})(\partial \xi/\partial \boldsymbol{x}') \cdot \mathcal{H} \cdot (\partial \xi/\partial \boldsymbol{x}')\rangle_{q,p_q}}{\langle (1/\sqrt{Z_\xi})\rangle_{q,p_q}} \tag{33}$$

This expression is identical to an expression derived by den Otter and Briels [28].

2.6. Comparison Between Quasistatic and Adaptive Biasing Force Approximations

Before closing this section we summarize the differences between SFM in the quasistatic approximation and SFM with Adaptive Biasing Force.

For SFM in the quasistatic approximation, ξ is decoupled from the other degrees of freedom by adding a force opposite to the force acting along ξ. Then an external force with zero mean is applied to ξ such that the motion of ξ is quasistatic. If we denote $-\lambda \nabla \xi$ the force acting along ξ and F^{qs} the force added to oppose it, we have (see Eq. (32))

$$F^{qs} = \lambda \nabla \xi$$

$$\frac{\partial A}{\partial \xi} = \frac{\langle (\lambda + G^{qs}/\sqrt{Z_\xi})\rangle}{\langle (1/\sqrt{Z_\xi})\rangle}$$

$$G^{qs} \overset{\text{def}}{=} \frac{1}{Z_\xi^2}\left(\frac{1}{\beta} + \frac{\dot{\xi}^2}{Z_\xi}\right)\frac{\partial \xi}{\partial \boldsymbol{x}'} \cdot \mathcal{H} \cdot \frac{\partial \xi}{\partial \boldsymbol{x}'}$$

In this case F^{qs} does not derive from a potential and the system is not Hamiltonian. This is why the quasistatic approximation is required.

For SFM with the adaptive biasing force, the external force, F^{abf}, is added to the system, and we have (see Eqs. (8) and (26))

$$F^{abf} = \langle \lambda + G^{abf} \rangle^{(n)} \nabla\xi$$

$$\frac{\partial A}{\partial \xi} = \langle \lambda + G^{abf} \rangle$$

$$G^{abf} \overset{\text{def}}{=} \frac{1}{Z_\xi^2} \frac{2}{\beta} \frac{\partial \xi}{\partial \boldsymbol{x}'} \cdot \mathcal{H} \cdot \frac{\partial \xi}{\partial \boldsymbol{x}'}$$

In this case F^{abf} converges to ∇A and the system converges to a Hamiltonian system.

3. APPLICATION – ISOMERIZATION OF 1,2-DICHLORO-ETHANE IN WATER

To test the performance of the SFM, we studied the rotation around the C—C bond in 1,2-dichloroethane (DCE) dissolved in water. Specifically, we calculated the potential of mean force, $A(\xi)$, as a function of the Cl—C—C—Cl torsional angle ξ. The same quantity was previously calculated for DCE in several different environments, including the gas phase, bulk water, bulk hexane and the water–hexane interface, using conventional methods [23–25]. In all environments, $A(\xi)$ exhibits local minima corresponding to the trans and gauche arrangements of the chlorine atoms. However, the relative stabilities of these two conformations and the free energy barrier that separates them change with environment. The trans conformation was found to be favored by 1.1 kcal/mol in the gas phase, whereas the gauche conformations were slightly favored in water (by 0.3 kcal/mol) [23, 24]. The shift of 1.4 kcal/mol stabilizing the gauche conformations in aqueous solutions can be attributed to strong, favorable interactions between these polar conformations and water. Note that the symmetrical, trans conformation has no permanent dipole moment. Also, the free energy barrier between the gauche and trans states increased from 3.5 kcal/mol in the gas phase to 4.4 kcal/mol in aqueous solution. This indicates that the solvent provides a considerable contribution to the potential of mean force around ξ.

The system studied consisted of one DCE molecule and 343 water molecules placed in a cubic box whose edge length was 21.73 Å. This corresponds to a water density of approximately 1 g/cm^3. Periodic boundary

conditions were applied in the three spatial directions. The water–water interactions were described by the TIP4P potential model [32]. For DCE, an all-atom, fully flexible model was used. This model was described in detail previously [23]. All intermolecular interactions were truncated smoothly with a cubic spline function between 8.0 and 8.5 Å. The cutoff for atoms of DCE was based on small, neutral groups.

The MD equations of motion were integrated using the velocity Verlet algorithm with a time step of 1 fs. The temperature of the system was 300 K. The bond and angular constraints were resolved using RATTLE [26]. The same algorithm was also used to calculate the force of constraint acting on ξ, whenever necessary. To generate configurations from the canonical ensemble the Martyna *et al.*, implementation [31] of the Nosé-Hoover algorithm was used.

Initially, we performed simulations of the system without any modifications in both microcanonical and canonical ensembles. $A(\xi)$ was obtained from a series of calculations, in which ξ was constrained by a harmonic potential in 2 overlapping windows. The MD trajectory for each window was 1.0 ns long. From this trajectory the probability distribution, $P(\xi)$, of finding DCE in a conformation defined by ξ was obtained and used to calculate $A(\xi)$ from Eq. (2).

The potential of mean force in the full range of ξ was generated by matching $A(\xi)$ in the overlapping regions of consecutive windows. This was required to ensure that $A(\xi)$ was a continuous function of ξ. Matching was done using the Weighted Histograms Method (WHAM) [33].

The potentials of mean force in the microcanonical and canonical ensembles were nearly identical, and were quite similar to those calculated previously using the same potential functions [23, 24]. Gauche and trans conformations were found to have nearly the same free energy, and were separated by a barrier 4.2 kcal/mol high. The profile in the canonical ensemble, shown in Figure 1, served as the reference to determine accuracy of the SFM. The statistical precision of these profiles was further confirmed by fitting a Fourier series to $A(\xi)$ and repeating the calculations using the series as the biasing potential. As expected, the potential of mean force so generated was flat. The same calculations were also used to estimate the rotational diffusion constant, D, needed for the Langevin term in the quasistatic implementation of SFM. This was done by calculating the velocity autocorrelation function and employing the formula:

$$D = \frac{1}{2}\int_0^\infty \langle v(0)v(t)\rangle \, dt$$

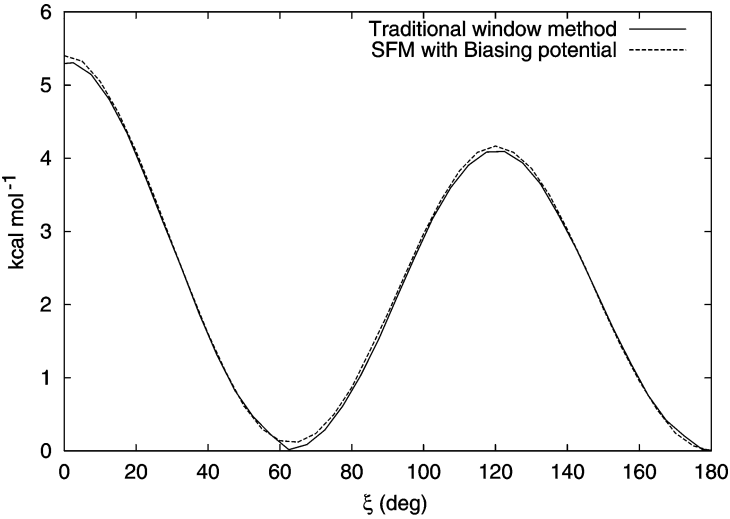

FIGURE 1 Free energy profile of the torsional angle, ξ, of DCE in bulk water calculated using the traditional window method and using the force acting on ξ in unconstrained simulation.

where $v(t)$ is the velocity of the torsional angle at time t and $\langle \ldots \rangle$ denotes a statistical average.

In the next step, we computed the potential of mean force using the force (Eq. (24)) rather than the probability density (Eq. (2)).

This simulation was carried out with the same biasing potential as in the previous case. At every MD step, the value of the constrained force, obtained using RATTLE, was binned in small intervals of ξ and, at the end of the simulation, the average value of the force of constraint in each bin was calculated. Next, these values were corrected for the geometrical factor according to Eq. (24), yielding the thermodynamic force as a function of ξ. This force was then integrated numerically to provide $A(\xi)$. The simulation was run for 1 ns and the resulting potential of mean force is shown in Figure 1. As can be seen, the agreement with the previously calculated profiles is excellent, confirming the correctness of Eq. (24).

3.1. Calculation of the Potential of Mean Force in the Quasistatic Approximation

In the next series of simulations the angle ξ was fully decoupled from the rest of the system. To advance this angle the Langevin equation of motion was

integrated. As shown in Section 2.4, the free energy of such a system should be calculated using Eq. (32).

It is expected that the potential of mean force along ξ converges to the exact solution only when ξ moves sufficiently slowly to obey the quasistatic approximation. Otherwise, the rest of the system cannot relax in response to motion along ξ, and the system is in a non-equilibrium state. Then the calculated free energy will be incorrect. To test the range of applicability of quasistatic approximation we performed simulations at four different values of diffusion coefficient in the Langevin equation. These values were $0.53\,\text{rad}^2/\text{ps}$, $0.053\,\text{rad}^2/\text{ps}$, $0.0053\,\text{rad}^2/\text{ps}$ and $0.0013\,\text{rad}^2/\text{ps}$. The first value is equal to the diffusion constant calculated for the Hamiltonian system with the biasing potential given by Eq. (5).

As can be seen in Figure 2, the free energy converges to the exact solution as D decreases. The accuracy of $A(\xi)$ for $\text{D} = 0.53\,\text{rad}^2/\text{ps}$ is unsatisfactory. The agreement with the exact solution improves markedly when D is lowered to $0.053\,\text{rad}^2/\text{ps}$, but the differences are not negligible. The error in calculating the free energy difference between gauche and trans states is $0.3-0.4$ kcal/mol, which is approximately equal to the thermal energy of $kT/2$. When the diffusion coefficient is further decreased, the calculated $A(\xi)$ becomes quite accurate (this would not be the case if Eq. (24) were used).

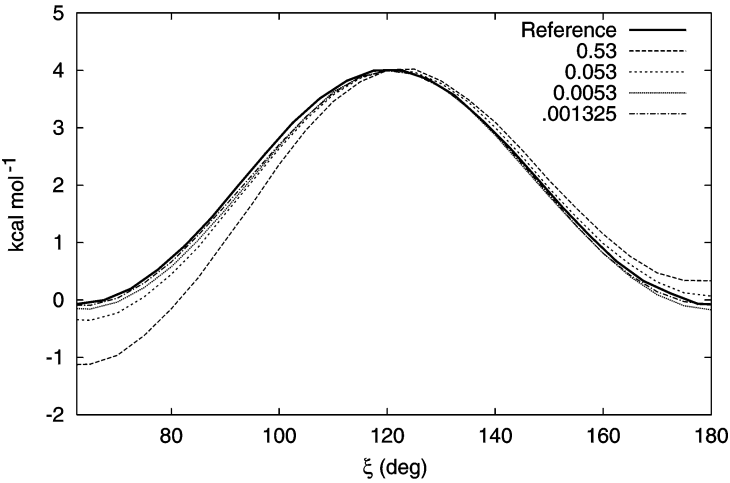

FIGURE 2 Free energy profile of the torsional angle of DCE in bulk water obtained from SFM in quasistatic approximation using Langevin force with diffusion coefficient, $\text{D} = 0.53$, 0.53×10^{-1}, 0.53×10^{-2} and $0.13 \times 10^{-2}\,\text{rad}^2/\text{ps}$. The reference curve is shown with the thick line. Only the range [60–180] degrees was computed. Note that since the free energy is defined to within a constant the curves were aligned at $\xi = 120$ deg.

There is, however, a price to pay. As D decreases, the simulation time increases and more windows are needed [13]. For $D = 0.53\,rad^2/ps$ and $0.053\,rad^2/ps$, a 1 ns MD trajectory in a single window was sufficient whereas for $D = 0.0053\,rad^2/ps$ and $0.0013\,rad^2/ps$, two and three windows were needed, respectively. In addition, the lengths of the MD trajectories were increased to 2 ns in the last case. It appears that, for the system considered here, $D = 0.053\,rad^2/ps$ offers the best balance between efficiency and accuracy.

3.2. SFM with Adaptive Biasing Force

MD simulation of DCE in bulk water using SFM with an adaptive biasing force was carried out in a single window of ξ extending from -20 deg to 200 deg. The length of the MD trajectory was 2 ns. Force statistics were collected in bins 5 deg wide. The number of sample points per bin was approximately 45,000, ranging from 40,022 samples to 50,149 samples.

In Figure 3 we compare $A(\xi)$ computed with the adaptive biasing force and using the traditional window method, as described above. The difference between the two profiles is within the statistical error bounds. $P(\xi)$ in the Adaptive Biasing Force simulation was found to be quite uniform, with oscillations not exceeding 12% around the mean. Thus, deviations from uniformity of $P(\xi)$ have only minor effect on the efficiency of sampling ξ.

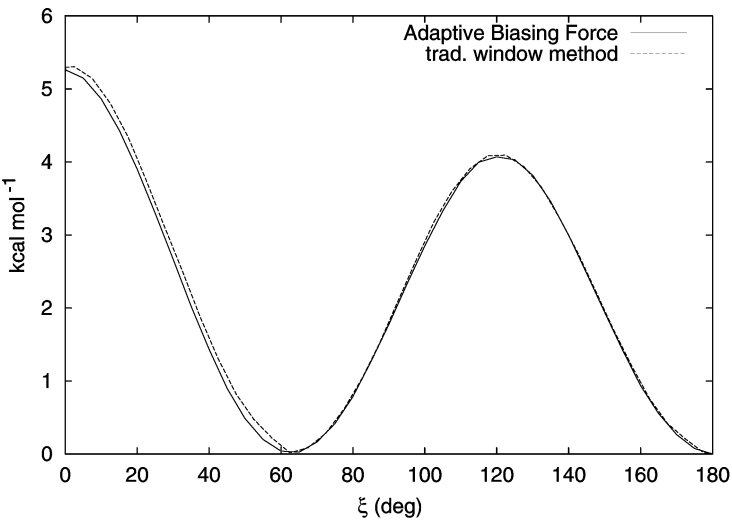

FIGURE 3 Free energy profile of the torsional angle of DCE in bulk water calculated using the traditional window method and the Adaptive Biasing Force method.

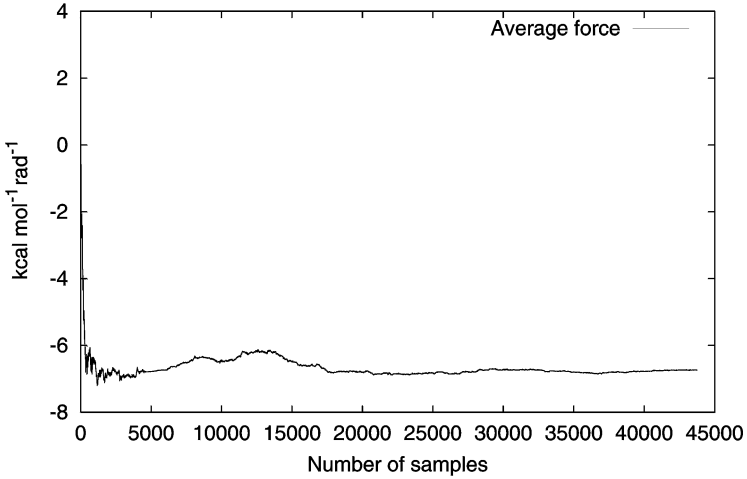

FIGURE 4 Calculated average force as a function of the number of samples in the interval of ξ between 35 deg and 40 deg.

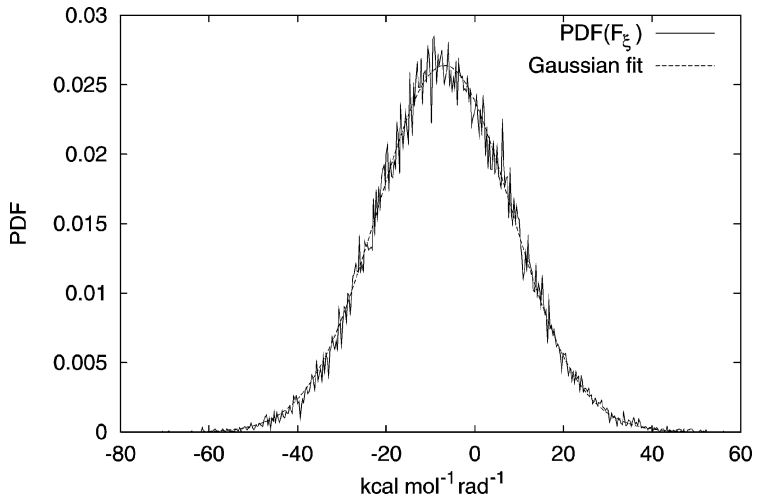

FIGURE 5 Probability distribution function of F_ξ for ξ in the interval between 35 deg and 40 deg, and a Gaussian fit to this probability distribution function.

In Figure 4 we show the convergence of $\langle F_\xi \rangle_{S_\xi}^{(n)}$ as a function of n (see Eq. (8)). These results are for the interval in ξ between 35 deg and 40 deg. As can be seen, convergence is quite rapid, which accounts for the very good performance of the method. This rapid convergence can be attributed to a

very simple structure of the probability distribution of the force F_ξ at a given location ξ. As shown in Figure 5, this distribution is nearly Gaussian.

4. DISCUSSION

In this paper, we develop a family of methods for calculating the free energy along a selected generalized coordinate, ξ, which rely on calculating the force acting on this coordinate. In the simplest of these methods, the system remains within the Hamiltonian framework. At each timestep, the instantaneous force acting on ξ is computed and is used to calculate the thermodynamic force. We provided details on how to implement this method by calculating the instantaneous force from, for example, the RATTLE algorithm. Note that this formula is different from the formula derived previously for constrained simulations [28]. Compared to the conventional method, which relies on calculating the probability distribution along ξ, the present approach is theoretically somewhat more involved. On the other hand, it has a useful advantage. When several windows are used, the conventional method requires matching the curves using, for example, WHAM (see Section 3). In our method no matching is required. Since the thermodynamic force is equal to the statistical average $\langle F_\xi \rangle$, the sampled values of F_ξ obtained from runs using different windows can simply be added to compute the final $\langle F_\xi \rangle$.

Both methods, mentioned above, suffer from the same disadvantage. To perform efficiently they require a good guess of the biasing potential. To avoid this difficulty and sample ξ efficiently (*i.e.*, uniformly or nearly uniformly) it is necessary to leave the Hamiltonian framework of the problem by subtracting (or, possibly, scaling) the force acting on ξ and substituting it by another force. We call this approach the Scaled Force Method. We explore two variants of this method, which asymptotically yield the exact free energy. In one approach the force along ξ is substituted by a force whose ensemble average is zero for all values of ξ. If motion along ξ is sufficiently slow that the quasistatic approximation applies, the thermodynamic force calculated along this coordinate yields a good estimate of the derivative of the free energy of the unmodified system. We provide the formula for making this estimate, which is not the same as the formula derived for the Hamiltonian system. In the specific implementation, adopted here, we use the Langevin equation of motion to advance ξ and examine when quasistatic approximation applies by changing diffusion coefficient. When D is set to the value calculated with the optimal biasing potential

(*i.e.*, a flat energy profile), we find that the quasistatic approximation is not accurate. When D is reduced by an order of magnitude, the error decreases to become approximately equal to the thermal energy. Further reductions of D reduce the error even more but, in the process, efficiency of the calculations suffers.

Alternatively, the instantaneous force acting on ξ can be modified using the current estimate of the average force at this value of ξ. This new force, calculated adaptively, converges to the correct average force as time goes to infinity and yields nearly uniform sampling of ξ. The method performs remarkably well yielding accurate estimates of the free energy. The success of this method appears to be related to the simple shape of the probability distribution of the forces acting on ξ which, in turn, allows the average force to be very quickly determined to good accuracy.

The Scaled Force Method is related to several other approaches to calculating the free energy. As has been already pointed out in the theory section, if we decouple ξ from the other degrees of freedom and the initial velocity along ξ is set to zero, the system will remain constrained to the initial value of ξ during the course of the simulation. If a series of simulations at different values of ξ were performed this would correspond exactly to the constrained force method [28]. Compared to methods based on unconstrained simulations, this approach has a well recognized deficiency that keeping some degrees of freedom fixed may impede sampling along other degrees of freedom. On the other hand, the constrained force method and SFM share the same advantage that they do not require prior knowledge of a biasing potential.

If there is a small, initial velocity along ξ, such that the quasistatic approximation is justified, then the approach can be considered to be a variant of the "slow growth" method [34, 35]. This method, however, is not expected to be accurate because it does not adequately sample the phase space. If a series of trajectories were to be obtained starting from a set of thermally representative configurations at some initial value of ξ, ξ_{init}, the formalism developed by Jarzynski would apply and the free energy could be, at least in principle, obtained accurately even without the requirement that quasistatic approximation applies [36, 37].

The Adaptive Biasing Force method is clearly related to the adaptive umbrella sampling algorithm [38, 39]. In this algorithm, the estimate of $U_b(\xi)$ is occasionally updated on the basis of $P(\xi)$ calculated from the most recent fragment of the trajectory. Eventually, $U_b(\xi)$ becomes sufficiently close to $A(\xi)$ that $P(\xi)$ is nearly constant. Compared to the Adaptive Biasing Force method, this approach has some disadvantages. First, a good initial

guess for $U_b(\xi)$ is still needed. Otherwise, some regions of ξ will be sampled poorly or not at all. Second, $U_b(\xi)$ can be updated only if sufficient statistics is accumulated in the full range of ξ or, at least, within one window. In contrast, the Adaptive Biasing Force method ensures that all regions of ξ are sampled, and the estimate of the biasing force in each bin of ξ is updated "on the fly", irrespective of the accuracy of estimates in other bins. One deficiency of the Adaptive Biasing Force method is that the system does not correspond precisely to a Hamiltonian system. In practice, this does not appear to be a problem. Moreover, updating the biasing force can be terminated at any time, if desired, and the most recent estimates of this force can be used for the rest of the simulation. This restores the Hamiltonian structure of the system.

The proposed methods are also conceptually related to multicanonical Monte Carlo method in the sense that both approaches are aimed at removing energy barriers in phase space. In the most common implementation of multicanonical Monte Carlo, phase space becomes flat, which is usually undesirable for systems containing many fast degrees of freedom, especially those associated with the solvent. Implementations, in which probability distribution is uniform only along selected degrees of freedom are possible, but may not be easy [10, 40].

Uniform sampling of slow degrees of freedom, which is desirable in free energy calculations, is usually not beneficial if the goal is to identify conformations of flexible molecules corresponding to local or global energy minima. Efficient methods to accomplish this goal usually rely on reducing free energy barriers rather than removing them completely. This requirement can be readily incorporated into the proposed method. Instead of completely removing the force acting on ξ we can scale it by a factor $0 < \alpha < 1$. Note that the system is unmodified when $\alpha = 1$, and ξ is completely decoupled from the rest of the system when $\alpha = 0$. In all intermediate cases, the free energy is approximately scaled by α. This corresponds to scaling the whole reduced phase space by α which, as required, leaves the positions of free energy minima in the same place as in the unmodified system. If needed, scaling can be generalized by making α a function of ξ or defining it in an adaptive fashion.

Much work still needs to be done to determine the full potential of SFM. First, the range of applicability and efficiency of the quasistatic approximation and the Adaptive Biasing Force method needs to be determined for a variety of systems. This includes examining different equations of motion for the slow coordinate in quasistatic approximation and different protocols for the Adaptive Biasing Force method. Perhaps more importantly, SFM

needs to be extended to a larger number of slow degrees of freedom, and tested in free energy calculations and in the search for minimum energy structures of flexible molecules.

A. APPENDIX – IMPLEMENTATION OF SCALED FORCE METHOD

A.1. Change of Variables in Multidimensional Integrals

We denote x, $\boldsymbol{p}_x$ the Cartesian coordinates and momenta. The set of generalized coordinates is denoted by $\xi, q_1, \ldots, q_{3N-1}$ and the momenta $p_\xi, p_{q_1}, \ldots, p_{q_{3N-1}}$. Recall that matrix J is defined as

$$J \stackrel{\text{def}}{=} \begin{pmatrix} (\partial\xi/\partial x_1) & (\partial\xi/\partial x_2) & \ldots & (\partial\xi/\partial x_{3N}) \\ (\partial q_1/\partial x_1) & (\partial q_1/\partial x_2) & \ldots & (\partial q_1/\partial x_{3N}) \\ \ldots & \ldots & \ldots & \ldots \\ (\partial q_{3N-1}/\partial x_1) & (\partial q_{3N-1}/\partial x_2) & \ldots & (\partial q_{3N-1}/\partial x_{3N}) \end{pmatrix}$$

See Eq. (9). Thus the Jacobian T of the transformation from Cartesian to generalized degrees of freedom (coordinates+momenta) is equal to:

$$T = \begin{pmatrix} J & 0 \\ * & (J^t)^{-1} \end{pmatrix}$$

The determinant of T is thus equal to:

$$|T| = |J|\,|(J^t)^{-1}| = 1$$

In particular we have:

$$\int \exp(-H/kT)\delta(\xi - \xi(\boldsymbol{x}))\, d\boldsymbol{x} d\boldsymbol{p}_x = \int \exp(-H/kT)\; dq_1 \ldots dq_{3N-1}\, dp_\xi dp_{q_1} \ldots dp_{q_{3N-1}} \tag{34}$$

A.2. External Force with Zero Mean

We chose to advance ξ using the Langevin equation of motion. This is a very simple choice and the implementation is quite straightforward. We define $\mu(t)$ with:

$$\mu(t) = -\zeta\dot{\xi} + R(t)$$

and

$$\langle R(t)R(t')\rangle = 2\zeta kT_\xi \delta(t-t')$$

where ζ is friction coefficient, $R(t)$ is normally distributed random force, whose ensemble average is zero, and T_ξ is the temperature. Note that ζ is related to the diffusion constant, D, by the Einstein relation:

$$D = kT/\zeta$$

The total external force applied to the system is equal to the RATTLE force plus the Langevin force:

$$\left(\lambda(t) + \frac{\mu(t)}{Z_\xi}\right)\frac{\partial \xi}{\partial \boldsymbol{x}}$$

Then $\ddot{\xi} = \mu(t)$. Numerical algorithm for advancing the Langevin equation of motion was described by Brooks *et al.* [41].

A.3. Calculation of Lagrange Multipliers Using RATTLE

At each timestep we need to calculate the force along ξ, which is of the form $\lambda(t)(\partial\xi/\partial x)$. This is the centerpiece of SFM. The force must be such that:

$$Z_\xi \lambda(t) - \frac{\partial \Phi}{\partial \boldsymbol{x}'}\cdot\frac{\partial \xi}{\partial \boldsymbol{x}'} + \boldsymbol{p}'_{\boldsymbol{x}}\cdot\mathcal{H}\cdot\boldsymbol{p}'_{\boldsymbol{x}} = 0$$

To compute the value of $\lambda(t)$ we use a modified version of RATTLE, for which the "constraints" are updated at each timestep.

Consider the traditional RATTLE algorithm and suppose that we have a constraint $\sigma(\boldsymbol{x}) = \sigma_0$, which has to be satisfied at each timestep. The algorithm consists of two steps. After advancing the position from time t to $t+dt$, RATTLE is used to compute the force $\mu^r\nabla\sigma$, such that $\sigma(\boldsymbol{x}(t+dt)) = \sigma_0$. After advancing the velocity from time $t+dt/2$ to $t+dt$, RATTLE is used to compute the force $\mu^v\nabla\sigma$, such that $v\cdot\nabla\sigma = 0$.

In contrast, in SFM we need to add a force which exactly compensates the acceleration of ξ due to the interatomic forces. Since the constraint has to be changed at each timestep the algorithm is slightly different. After advancing the position from time t to $t+dt$, RATTLE is used to compute the force $\lambda^r\nabla\xi$, such that $\xi(t+dt) = \xi(t) + dt\,\dot{\xi}(t)$, where $\dot{\xi}(t)$ is the velocity before the forces are applied at time t. After advancing the velocity from time $t+dt/2$ to $t+dt$, RATTLE is used to compute the force $\lambda^v\nabla\xi$, such

that $v \cdot \nabla\xi(t+dt) = \dot{\xi}(t+dt) = \dot{\xi}(t)$, where $\dot{\xi}(t)$ is the velocity before the forces are applied at time t.

To complete the description of the modified RATTLE algorithm we derive the equations for λ^r and λ^v, the position and velocity Lagrange multipliers in RATTLE. The derivation is done assuming that no external force is applied to ξ, but the results hold for any external force applied.

Let us consider the position RATTLE. The position is advanced using:

$$r(t+dt) = r(t) + v(t+dt/2)dt \tag{35}$$

while the velocity is advanced using:

$$v(t+dt/2) = v(t) + \frac{dt}{2}\frac{F(t)}{m} \tag{36}$$

in "condensed" notations.

After position RATTLE is applied, we want ξ to be equal to:

$$\xi^R(t+dt) = \xi(t) + dt\dot{\xi}(t) \tag{37}$$

We expand $\xi^R(t+dt)$ using the Taylor series and use Eqs. (35) and (36), with Definitions (10) of Z_ξ, and (15) of $\mathcal{H}$. This yields:

$$\begin{aligned}
\xi^R(t+dt) &= \xi\left(r(t+dt) + dt\ \lambda^r \frac{\nabla\xi}{m}\right) \\
&= \xi\left(r(t) + dt\ v(t) + \frac{dt^2}{2}\frac{F(t)}{m} + dt\ \lambda^r \frac{\nabla\xi}{m}\right) \\
&= \xi(t) + dt\ \dot{\xi}(t) + \frac{dt^2}{2}\frac{F(t)}{m}\nabla\xi + dt\ Z_\xi \lambda^r \frac{dt^2}{2} v(t)\cdot\mathcal{H}\cdot v(t)
\end{aligned}$$

Using Eq. (37) we obtain the equation for λ^r:

$$\lambda^r(t) = \frac{-dt}{2Z_\xi(t)}\left(\frac{F(t)}{m}\nabla\xi + v(t)\cdot\mathcal{H}\cdot v(t)\right) = \frac{dt}{2}\frac{-\ddot{\xi}(t)}{Z_\xi} \tag{38}$$

Thus $\lambda^r(t)$ can be used to evaluate numerically $\ddot{\xi}(t)$.

For velocity RATTLE we have a similar equation. For the velocity:

$$v(t+dt) = v(t) + \frac{dt}{2}\frac{F(t)}{m} + \lambda^r\frac{\nabla\xi(t)}{m} + \frac{dt}{2}\frac{F(t+dt)}{m} \tag{39}$$

$$v^R(t+dt) = v(t+dt) + \lambda^v\frac{\nabla\xi(t+dt)}{m} \tag{40}$$

The constraint on $v^R(t+dt)$ is

$$\nabla\xi(t+dt)\cdot v^R(t+dt) = \nabla\xi(t)\cdot v(t) \tag{41}$$

since we assume that no additional (*e.g.*, Langevin) force is applied.

Using Eqs. (39), (40) and (41):

$$dt\, v(t)\cdot\mathcal{H}\cdot v(t)+\nabla\xi(t+dt)\left(\frac{dtF(t)}{2}\frac{}{m}+\lambda^r\frac{\nabla\xi(t)}{m}+\frac{dtF(t+dt)}{2}\frac{}{m}+\lambda^v\frac{\nabla\xi(t+dt)}{m}\right)=0$$

Thus:

$$\lambda^v=\frac{-dt}{2Z_\xi(t+dt)}\left(\frac{F(t)}{m}\nabla\xi+\frac{2}{dt}\lambda^r\frac{\nabla\xi(t)\cdot\nabla\xi(t+dt)}{m}+\frac{F(t+dt)}{m}\nabla\xi+2v\cdot\mathcal{H}\cdot v\right)$$

Using Eq. (38) we obtain the first order approximation:

$$\begin{aligned}\lambda^v(t) &= \frac{-dt}{2Z_\xi(t+dt)}\left(\frac{F(t)}{m}\nabla\xi+\frac{2Z_\xi(t)}{dt}\lambda^r+\frac{F(t+dt)}{m}\nabla\xi+2v\cdot\mathcal{H}\cdot v\right)\\ &= \frac{-dt}{2Z_\xi(t+dt)}\left(\frac{F(t+dt)}{m}\nabla\xi+v(t)\cdot\mathcal{H}\cdot v(t)\right)\end{aligned}$$

while λ^r and λ^v are equal up to second order in dt^2, λ^r includes higher order terms obtained through an iterative procedure. Numerical tests suggest that using $2\lambda^r$ rather than $\lambda^r+\lambda^v$ or $2\lambda^v$ yields a more accurate result for the average force and free energy.

A.4. Implementation of Velocity Verlet Algorithm with Nose-Hoover Thermostat

Notations

r	Position before RATTLE
r^R	Position after RATTLE
v	Velocity at time t
v^{th}	Velocity after thermostat
v^{La}	Velocity after Langevin force
v^{F_1}	Velocity after inter-atomic forces
v^{RP}	Velocity after Position RATTLE
v^{F_2}	Velocity after second application of inter-atomic forces
v^{RV}	Velocity after Velocity RATTLE

v^{ξ} Projection of v on $\nabla\xi$
$\dot{\xi}^{\text{ref}}$ Velocity of ξ after Langevin force
$\dot{\xi}^{F_1}$ Velocity of ξ after inter-atomic forces
$\dot{\xi}^{RP}$ Velocity of ξ after Position RATTLE
$\dot{\xi}^{F_2}$ Velocity of ξ after second application of inter-atomic forces
$\dot{\xi}^{RV}$ Velocity of ξ after Velocity RATTLE
F inter-atomic forces
F^{La} Langevin force
G^{p} Position RATTLE force
G^{V} Velocity RATTLE force
η thermostat

We describe the complete, step-by-step algorithm. The reader should not be confused by the nine steps of the method. These steps correspond to a conventional implementation of this algorithm in MD. The only difference is that RATTLE is implemented in SFM using varying "constraints", updated at each time-step (steps 2 and 9).

In this presentation we chose the Langevin force to advance ξ. Other choices may be made. Also, the full scaling of the thermodynamics force is applied. The scheme with intermediate scaling ($0 < \alpha < 1$) can be easily derived.

(1) Add contributions from interatomic forces:

$$v^{F_2}(t - dt/2) = v^{RP}(t - dt/2) + \frac{dt}{2m}F(t)$$
$$\dot{x}^{F_2}(t - dt/2) = v^{F_2}(t - dt/2) \cdot \nabla\xi^{R}(t)$$

(2) Apply the velocity part of RATTLE. The target value for the reaction coordinate, ξ is:

$$\dot{\xi}^{RV}(t - dt/2) = \dot{\xi}^{\text{ref}}(t - dt/2)$$

New velocity:

$$v^{RV}(t - dt/2) = v^{F_2}(t - dt/2) + \frac{dt}{2m}G^{V}(t)$$

(3) Advance ξ using the external force.

$$v^{La}(t) = v^{RV}(t - dt/2) + \frac{dt}{2m}F^{La}(t)$$

(4) Apply thermostat to the system. No thermostat is applied to ξ.

4-a. Advance thermostat from $t-dt/2$ to t using low order approximation:

$$\eta(t) = \eta(t - dt/2) + \frac{dt}{2Q}[m(v^{La}(t) - v^{\xi}(t))^2 - (N-1)\kappa T]$$
$$v(t) = v^{La}(t) - \frac{dt}{2}\eta(t)(v^{La}(t) - v^{\xi}(t))$$

where

$$v^{\xi} = \frac{\dot{\xi}}{Z_{\xi}}\left(\frac{1}{m_i}\frac{\partial \xi}{\partial x_i}\right)$$

4-b. Iterate thermostat and velocity using high-order approximation:

$$\eta = \eta(t - dt/2) + \frac{dt}{2Q}[m(v - v^{\xi})^2 - (N-1)\kappa T]$$
$$v = v^{La}(t) - \frac{dt}{2}\eta(v - v^{\xi})$$

(5) Advance velocity and thermostat at time t:

$$v^{th}(t) = v(t) - \frac{dt}{2}\eta(t)(v(t) - v^{\xi}(t))$$
$$\eta(t + dt/2) = \eta(t) + \frac{dt}{2Q}[m(v - v^{\xi})^2 - (N-1)\kappa T]$$

(6) Advance ξ using the external force.

$$v^{La}(t + dt/2) = v^{th}(t) + \frac{dt}{2m}F^{La}(t)$$
$$\dot{\xi}^{\text{ref}}(t + dt/2) = v^{La}(t + dt/2) \cdot \nabla \xi^{R}(t)$$

(7) Add contributions from interatomic forces:

$$v^{F_1}(t + dt/2) = v^{La}(t + dt/2) + \frac{dt}{2m}F(t)$$
$$\dot{\xi}^{F_1}(t + dt/2) = v^{F_1}(t + dt/2) \cdot \nabla \xi^{R}(t)$$

(8) Advance position:

$$r(t + dt) = r^{R}(t) + dt\ v^{F_1}(t + dt/2)$$

(9) Apply the position part of RATTLE. The target value for the reaction coordinate is:

$$\xi^R(t+dt) = \xi^R(t) + dt\ \dot{\xi}^{\text{ref}}(t+dt/2)$$

New position and velocity:

$$r^R(t+dt) = r(t+dt) + \frac{dt^2}{2m} G^P(t)$$
$$v^{RP}(t+dt/2) = v^{F_1}(t+dt/2) + \frac{dt}{2m} G^P(t)$$
$$\dot{\xi}^{RP}(t+dt/2) = v^{RP}(t+dt/2) \cdot \nabla \xi^R(t+dt)$$

References

[1] Frenkel, D. and Smit, B., *Understanding Molecular Simulations*, Academic Press, San Diego, 1986.

[2] Vlugt, T. J. H., Martin, M. G., Smit, B., Siepmann, J. I. and Krishna, R. (1998). "Improving the efficiency of the configurational-bias Monte Carlo algorithm", *Mol. Phys.*, **94**, 727.

[3] Berne, B. J. and Straub, J. E. (1997). "Novel methods of sampling phase space in the simulation of biological systems", *Curr. Opin. Struct. Biol.*, **7**, 181.

[4] Huo, S. and Straub, J. E. (1999). "Direct computation of long time processes in peptides and proteins: reaction path study of the coil-to-helix transition in polyalanine", *Proteins: Structure, Function and Genetics*, **36**, 249.

[5] Frantz, D. D., Freeman, D. L. and Doll, J. D. (1990). "Reducing quasi-ergodic behavior in Monte Carlo simulations by J-walking: applications to atomic clusters", *J. Chem. Phys.*, **93**, 2769.

[6] Curotto, E., Freeman, D. L. and Doll, J. D. (1998). "A j-walking algorithm for micro-canonical simulations: applications to Lennard-Jones clusters", *J. Chem. Phys.*, **109**, 1643.

[7] Xia, Y., Huang, E. S., Levitt, M. and Samudrala, R. (2000). "*Ab Initio* construction of protein tertiary structures using a hierarchical approach", *J. Mol. Biol.*, **300**, 171.

[8] Wong, K.-B., Clarke, J., Bond, C. J., Niera, J. L., Freund, S. M. V., Fersht, A. R. and Daggett, V. (2000). "Towards a complete description of the structural and dynamic properties of the denatured state of Barnase and the role of residual structure in folding", *J. Mol. Biol.*, **296**, 1257.

[9] Alonso, D. O. V. and Daggett, V. (2000). "Staphylococcal protein A: Unfolding pathways, unfolded states, and differences between the B and E domains", *Proc. Nat. Acac. Sci. USA*, **97**, 133.

[10] Janke, W. (1998). "Multicanonical Monte Carlo simulations", *Physica A*, **254**, 164.

[11] Mitsutake, A. and Okamoto, Y. (2000). "Helix-coil transitions of amino-acid homo-oligomers in aqueous solution studied by multicanonical simulations", *J. Chem. Phys.*, **112**, 10638.

[12] Torrie, G. M. and Valleau, J. P. (1977). "Nonphysical sampling distributions in Monte Carlo free energy estimation: Umbrella sampling", *J. Comput. Phys.*, **23**, 187.

[13] Chandler, D., *Introduction to Modern Statistical Mechanics*, Oxford University Press, Oxford, 1987.

[14] Marrink, S. J. and Berendsen, H. J. C. (1994). "Simulation of water transport through a lipid membrane", *J. Phys. Chem.*, **98**, 4155.

[15] Wilson, M. A. and Pohorille, A. (1996). "Mechanism of unassisted ion transport across membrane bilayers", *J. Am. Chem. Soc.*, **118**, 6580.

[16] Pohorille, A., Wilson, M. A., Chipot, C., New, M. H. and Schweighofer, K. S., "Interactions of small molecules and peptides with membranes", In: *Computational Molecular Biology*, *Theoretical and Computational Chemistry*, Lesczynski, J., Ed., Elsevier, Amsterdam, 1999, pp. 485–526.
[17] Boczko, E. M. and Brooks III, C. L. (1995). "First principles calculation of the folding free energy of a three-helix bundle protein", *Science*, **269**, 393.
[18] Jorgensen, W. L. (1981). "Internal rotation in liquid 1,2-dichloroethane and *n*-butane", *J. Am. Chem. Soc.*, **103**, 677.
[19] Jorgensen, W. L., Binning, R. C. Jr. and Bigot, B. (1981). "Structure and properties of organic liquids: *n*-butane and 1,2-dichloroethane and their conformational equilibria", *J. Am. Chem. Soc.*, **103**, 4393.
[20] Millot, C. and Rivail, J. P. (1992). "Molecular dynamics simulation of the TIPS model of 1,2-dichloroethane in the liquid phase", *Mol. Phys.*, **77**, 157.
[21] Depaepe, J.-M. and Ryckaert, J.-P. (1995). "Isomerization of 1,2-dichloroethane in polar nad non-polar solvents", *Chem. Phys. Lett.*, **245**, 653.
[22] Vilaseca, E. (1996). "Solvent effect on conformational equilibrium: a Monte Carlo study of 1,2-dichloroethane in carbon tetrachloride", *J. Chem. Phys.*, **104**, 4243.
[23] Benjamin, I. and Pohorille, A. (1993). "Isomerization reaction dynamics and equilibrium at the liquid–vapor interface of water – a molecular dynamics study", *J. Chem. Phys.*, **98**, 236.
[24] Pohorille, A. and Wilson, M. A., "Isomerization reactions at aqueous interfaces", In: *Reaction Dynamics in Clusters and Condensed Phases – The Jerusalem Symposia on Quantum Chemistry and Biochemistry*, **26**, Jortner, J., Levine, R. D. and Pullman, B., Eds., Kluwer, Dordrecht, 1993, pp. 207–227.
[25] Jorgensen, W. L., McDonald, N. A., Selmi, M. and Rablen, P. R. (1995). "Importance of polarization for dipolar solutes in low-dielectric media – 1,2-dichloroethane and water in cyclohexane", *J. Am. Chem. Soc.*, **117**, 11809.
[26] Andersen, H. C. (1983). "RATTLE: a 'velocity' version of the SHAKE algorithm for molecular dynamics calculations", *J. Comput. Phys.*, **52**, 24.
[27] Allen, M. P. and Tildesley, D. J., *Computer Simulation of Liquids*, Oxford University Press, Oxford, 1987.
[28] den Otter, W. K. and Briels, W. J. (1998). "The calculation of free-energy differences by constrained molecular-dynamics simulation", *J. Chem. Phys.*, **109**, 4139.
[29] Nosé, S. (1984). "A molecular dynamics method for simulations in the canonical ensemble", *Mol. Phys.*, **52**, 255.
[30] Hoover, W. G. (1985). "Canonical dynamics: equilibrium phase space distributions", *Phys. Rev. A*, **31**, 1695.
[31] Martyna, G. J., Klein, M. L. and Tuckerman, M. (1992). "Nose-Hoover chains – the canonical ensemble *via* continuous dynamics", *J. Chem. Phys.*, **97**, 2635.
[32] Jorgensen, W. L., Chandrasekhar, J., Madura, J. D., Impey, R. W. and Klein, M. L. (1983). "Comparison of simple potential functions for simulating liquid water", *J. Chem. Phys.*, **79**, 926.
[33] Kumar, S., Bouzida, D., Swendsen, R. H., Kollman, P. A. and Rosenberg, J. M. (1992). "The weighted histogram analysis method for free-energy calculations on biomolecules 1: the method", *J. Comput. Chem.*, **13**, 1011.
[34] Straatsma, T. P., Berendsen, H. J. C. and Postma, J. P. M. (1986). "Free energy of hydrophobic hydration: a molecular dynamics study of noble gasses in water", *J. Chem. Phys.*, **85**, 6720.
[35] Singh, U. C., Brown, F. K., Bash, P. A. and Kollman, P. A. (1987). "An approach to the application of free energy perturbation methods using molecular dynamics: applications to the transformations of $CH_3OH \rightarrow CH_3CH_3$, $H_3O^+ \rightarrow NH_4^+$, glycine $\rightarrow$ alanine, and alanine $\rightarrow$ phenylalanine in aqueous solution and to $H_3O^+ \rightarrow NH_4(H_2O)_3$ in the gas phase", *J. Am. Chem. Soc.*, **109**, 1607.
[36] Jarzynski, C. (1997). "Nonequilibrium equality for free energy differences", *Phys. Rev. Lett.*, **78**, 2690.
[37] Jarzynski, C. (1997). "Equilibrium free-energy differences from nonequilibrium measurements: A master-equation approach", *Phys. Rev. E*, **56**, 5018.

[38] Hooft, R. W. W., van Eijck, B. P. and Kroon, J. (1992). "An adaptive umbrella sampling procedure in conformational analysis using molecular dynamics and its application to glycol", *J. Chem. Phys.*, **97**, 6690.
[39] Bartels, C. and Karplus, M. (1998). "Probability distributions for complex systems: Adaptive umbrella sampling of the potential energy", *J. Phys. Chem. B*, **102**, 865.
[40] Higo, J., Nakajima, N., Shirai, H., Kidera, A. and Nakamura, H. (1997). "Two-component multicanonical Monte Carlo method for effective conformational sampling", *J. Comput. Chem.*, **18**, 2086.
[41] Pastor, R. W., Brooks, B. R. and Szabo, A. (1988). "An analysis of the accuracy of Langevin and molecular dynamics algorithms", *Mol. Phys.*, **65**, 1409.